

## Article

# Classification of Typical Tectonic Styles and Exploration of Hydrocarbon Accumulation Patterns in Southern Junggar Basin, China

Dongsheng Ji <sup>1</sup>, Yanan Xu <sup>1</sup>, Zhichao Pang <sup>1</sup>, Bo Yuan <sup>1</sup> and Kang Zhao <sup>2,\*</sup>

<sup>1</sup> Research Institute of Exploration and Development, Xinjiang Oilfield Company, PetroChina, Urumqi 830000, China

<sup>2</sup> School of Geosciences, Yangtze University, Wuhan 430100, China

\* Correspondence: 201671302@yangtzeu.edu.cn

**Abstract:** Affected by Tianshan uplift, the southern Junggar Basin has experienced multi-stage tectonic movements and formed many large-scale anticlines with zonal distribution. The key to hydrocarbon exploration is to accurately implement anticline traps. This paper is guided by the fault-related folds theory to tectonically interpret several seismic profiles in the southern Junggar Basin and then summarize the anticline types and their hydrocarbon accumulation characteristics. This paper showed that the southern Junggar Basin has a tectonic assemblage pattern of “multi-detachment layers and multi-phase superposition”. According to the superimposed shape of the anticlines, they could be divided into overthrust anticlines, compound anticlines and multiple superimposed anticlines, and the horizontal and vertical positions of the different types of anticlines are different. The hydrocarbon accumulating characteristics of the different types of anticlines are shown to be different. The highs of the overthrust anticlines and compound anticlines are stable, and the degree of exploration is relatively high. Although the degree of exploration of multiple overlapping anticlines is low, multiple layers can be exploited simultaneously in the process of oil development, with great hydrocarbon potential. The characteristics of hydrocarbon accumulation in the southern Junggar Basin are discussed in order to provide guidance for efficient hydrocarbon exploration.

**Keywords:** tectonic style; hydrocarbon accumulation characteristics; hydrocarbon reservoir assemblage; southern Junggar Basin; northern piedmont of Tianshan Mountains



**Citation:** Ji, D.; Xu, Y.; Pang, Z.; Yuan, B.; Zhao, K. Classification of Typical Tectonic Styles and Exploration of Hydrocarbon Accumulation Patterns in Southern Junggar Basin, China. *Energies* **2022**, *15*, 6715. <https://doi.org/10.3390/en15186715>

Academic Editor: Reza Rezaee

Received: 21 July 2022

Accepted: 12 September 2022

Published: 14 September 2022

**Publisher's Note:** MDPI stays neutral with regard to jurisdictional claims in published maps and institutional affiliations.



**Copyright:** © 2022 by the authors. Licensee MDPI, Basel, Switzerland. This article is an open access article distributed under the terms and conditions of the Creative Commons Attribution (CC BY) license (<https://creativecommons.org/licenses/by/4.0/>).

## 1. Introduction

The southern margin of the Junggar foreland basin at the northern foot of the Tianshan Mountains has attracted much attention due to its rich surface oil and gas seedlings and large-scale anticlines distributed in belts. The Jurassic and Lower Cretaceous strata in the southern Junggar foreland basin are the last anticline groups that have not been explored on a large scale in China [1,2]. In 2019, the Cretaceous Qingshuihe Formation of well Gaotan 1, located in the Gaoquan anticline, had a daily oil production of 1213 m<sup>3</sup> and gas production of 321,700 m<sup>3</sup>. In 2020, the Cretaceous Qingshuihe Formation of well Hutan 1, located in the Hutubi anticline, had a daily oil production of 106.5 m<sup>3</sup> and gas production of 619,000 m<sup>3</sup>. The discovery of these two wells with high hydrocarbon production confirmed that the southern Junggar Basin has the petroleum geological conditions for the formation of large oil and gas fields. Controlled by Tianshan uplift, three rows of anticlines were developed in the southern Junggar Basin [1,3–9]. Predecessors have carried out a large number of studies on tectonic interpretation, sedimentary reservoir and oil and gas accumulation for each anticline belt [2,7,10–13], which has played an important role in understanding the characteristics of the anticlines in the south of the Junggar Basin and guiding hydrocarbon exploration.

Due to multi-stage and multi-layer compression as well as thrusting and detachment, the deformations generated have spatial differences [3–6,14–18], that is, the anticline not

only has zonation in the plane but also has periodicity in the vertical direction. However, this vertical periodicity has not been paid enough attention to, and the coupling relationship between these anticlines and strata has not been studied. The above problems seriously restrict the three-dimensional analysis and hydrocarbon exploration of the anticlines in the southern Junggar Basin. The Upper Cretaceous and Tertiary were the main exploration strata before 2008, and the Jurassic and Lower Cretaceous became the key exploration strata after 2008. As the anticlines that occurred in the Jurassic and Lower Cretaceous period are the key targets of exploration, the Jurassic and Lower Cretaceous strata are the target stratigraphy of this paper. We used the latest 3D seismic data to summarize the vertical combination types of anticlines and then discussed the characteristics of oil and gas accumulation. This paper is expected to provide geological guidance for the efficient exploration of oil and gas in the Jurassic and Lower Cretaceous strata.

## 2. Geological Setting

The Junggar Basin, located in northwestern China (Figure 1a), is an important petroliferous basin with an area of about 134,000 km<sup>2</sup> [2,3,17]. Based on gravity and seismic data, the Junggar Basin can be divided into six primary tectonic units [17,18], including three uplifts, two depressions and one fold thrust belt (Figure 1b). The Junggar Basin has undergone five extension to compression stages of tectonic evolution since the Permian [17]. The southern Junggar Basin is located at the northern foot of the Tianshan Mountains. Its formation and evolution are closely controlled by the northern Tianshan tectonic belt. It has experienced the evolution stages of the Triassic Paleogene intracontinental depression and Neogene quaternary foreland basin [17–19]. Three rows of anticline tectonic belts extending nearly east-west were developed from south to north (Figure 1c).

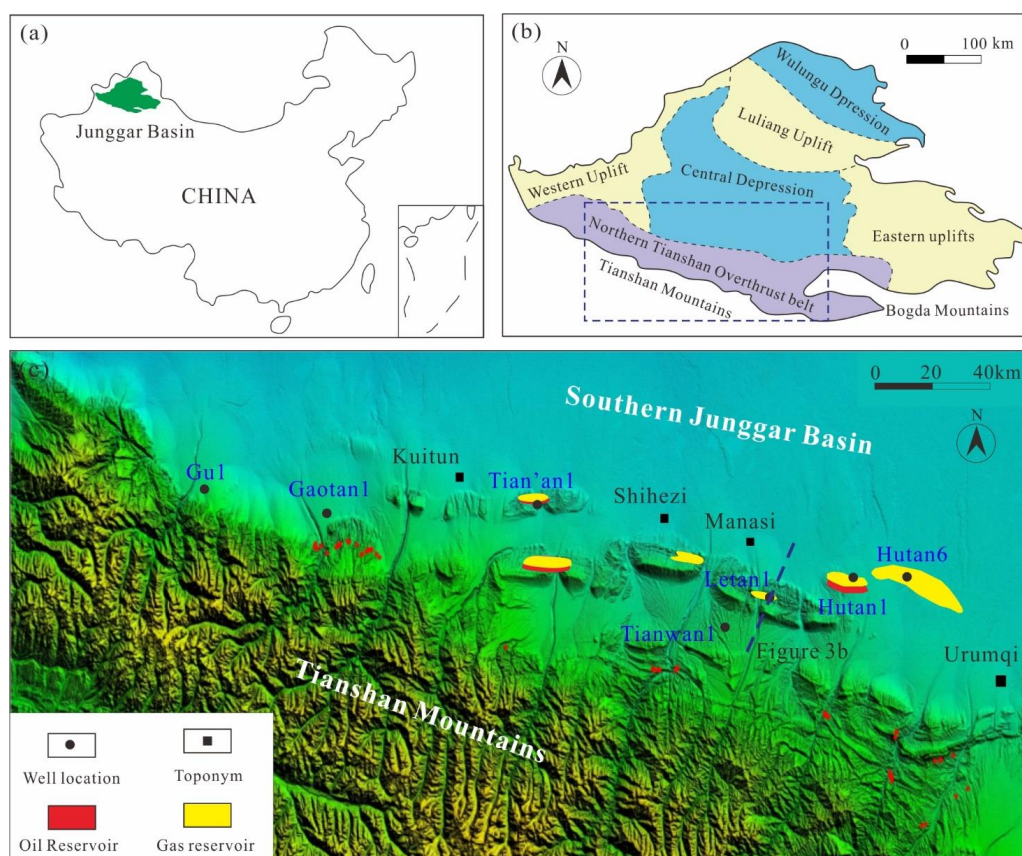


**Figure 1.** (a) Map of the Junggar Basin in China; (b) the division of tectonic units in the Junggar Basin and the location of southern Junggar Basin; (c) digital elevation model of the southern Junggar Basin.

Exploration has shown that there are three vertical petroleum systems [8,20]. The Upper Petroleum System refers to the reservoir and cap rock assemblage composed of the Miocene Shawan Formation and Tasihe Formation. The Middle Petroleum System refers to the reservoir and cap rock assemblage composed of the Upper Cretaceous and Paleogene strata. The Lower Petroleum System refers to the reservoir and cap rock assemblage composed of the Jurassic and Lower Cretaceous strata (Figure 2).

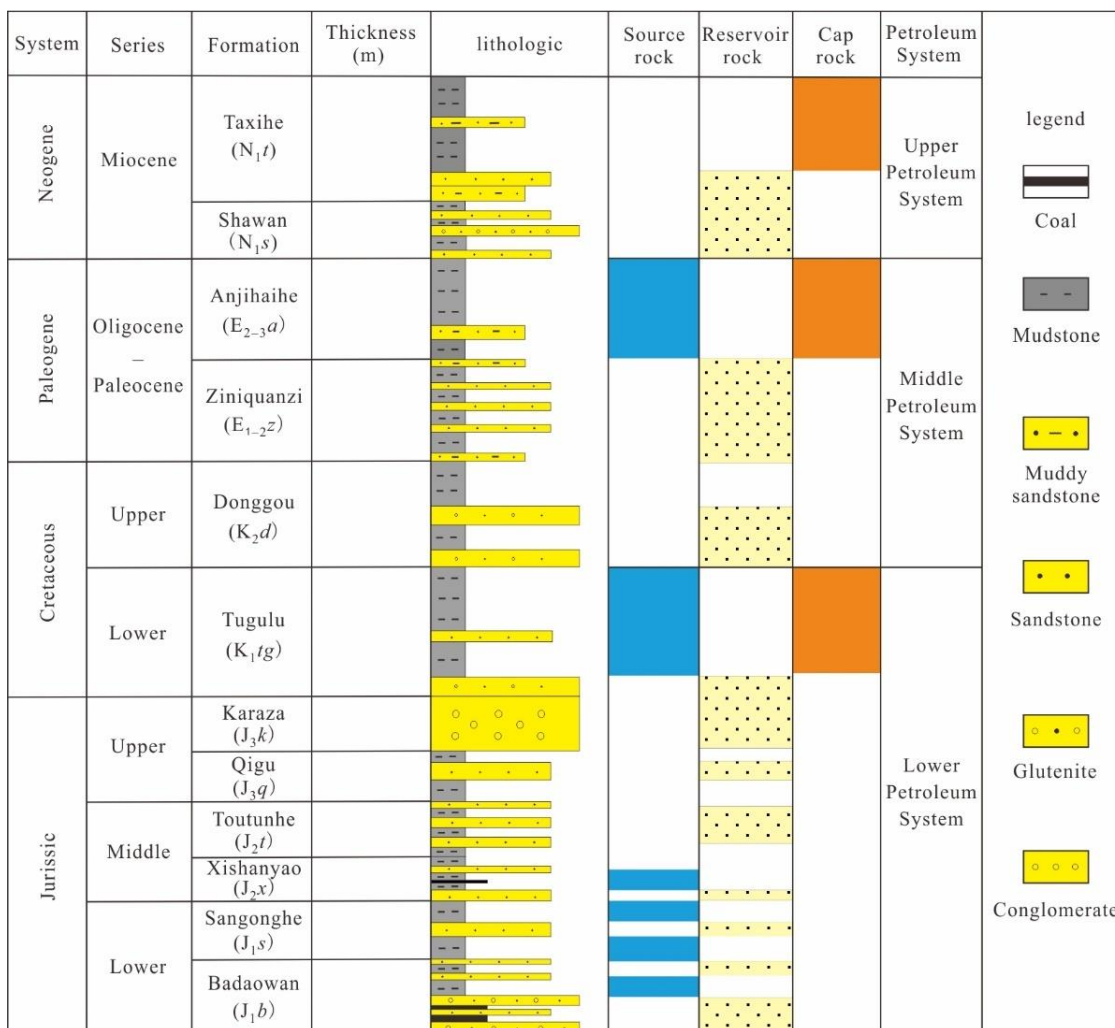


Figure 2. Comprehensive stratigraphic histogram.

The southern Junggar Basin has great potential for hydrocarbon. Five sets of source rocks of the Permian, Triassic, Jurassic, Cretaceous and Lower Tertiary Anjihaihe Formation were developed vertically, among which three sets of source rocks of the Jurassic, Cretaceous and Lower Tertiary Anjihaihe formation have been confirmed [21–29]. In particular, Jurassic source rocks are thick and widely distributed and are the main hydrocarbon-generating strata in the southern margin of Junggar Basin [30,31].

### 3. Data and Methods

This study relied on newly collected and partially reprocessed 2D seismic sections and 3D seismic data basis, as well as drilling and logging data from exploration wells. All these data were acquired by the PetroChina Xinjiang Oilfield Company. The large-scale regional 2D seismic profiles in this study were from a combination of different 2D seismic profiles within the basin. The dominant frequency of the seismic data was 28 Hz. Over the last decade, due to oil and gas exploration, dozens of wells have been drilled and

extensive lithological and logging data have been collected. In order to systematically study the lithology of the southern Junggar Basin, several wells with large drilling depths were selected for this study, while ensuring that detailed lithology and logging data were available for each major tectonic unit.

The mechanical parameters of a rock, such as shear modulus, bulk modulus, uniaxial compressive strength and inherent shear strength, were obtained by calculating the Poisson ratio, elastic modulus and shale content index through the acoustic logging and gamma logging data of the drilled wells in the target area [32,33]. From this, the rock's mechanical structure of the thick mudstone caprock was finely characterized, so as to determine the slippage layer. The layers not encountered by drilling were calculated based on the area-depth technique to determine the detachment layer. The area-depth technique is widely used to test the rationality of tectonic interpretation, predict the depth of the slippage layer and calculate the slip distance of the slippage layer, which is an effective method to study deep deformation based on shallow information [34–37].

All seismic and well data interpretation was completed using LandMark software. In order to establish the seismic data–well ties, 1D synthetic seismograms were first produced using acoustic and density curves and a convolution model. Then, the correlation between the synthetic seismogram and the real seismic section was analyzed, and finally, marked seismic events corresponding to the key stratigraphic interfaces were noted. In the southern Junggar Basin, two sets of obvious reflections were used as important marker beds for seismic data–well ties: one corresponds to the regional conglomerate layer in the bottom of the Cretaceous Tugulu Formation, and the other is associated with the coal seam in the Jurassic Xishanyao Formation [17].

One balanced cross-section was produced using 2D Move software based on the interpretation of the regional 2D seismic data. The location of the cross-section is shown in Figure 1c. The cross-section was perpendicular to the main structural orientation. A time-depth fitting equation was established. The restoration was performed mainly using line-length balancing in 2D Move.

In this paper, a large number of previous tectonic analysis research results and understandings were extensively investigated [1–13,17,18]. Then, using 2D seismic sections and 3D seismic data as research material, we used the tectonic geometric analysis method and balanced cross-section recovery technology and also considered the kinematic characteristics to carry out a tectonic interpretation of the main compound anticlines in the southern Junggar basin. On this basis, the anticline style in the southern Junggar Basin is divided according to the tectonic superposition relationship and stages of different strata.

## 4. Results

The typical tectonic styles in the southern Junggar Basin are classified according to the superimposed relationship and stages of tectonics, and then the characteristics of each tectonic style are described.

### 4.1. Classification of Typical Tectonic Styles in Southern Junggar Basin

The inherent shear strength of the Cretaceous Hutubi Formation mudstone is 2.0–6.0 MPa, and that of the Paleogene Anjihaihe Formation mudstone is 6.2 MPa. The two sets of mudstones have low inherent shear strength and are good regional detachment layers (Figure 3a). According to the area-depth technique, it is considered that a detachment layer also developed in the Triassic, and the depth of the detachment layer is about 9 km. Overpressures also widely occurred in the Jurassic source rocks. The source rocks have anomalously high acoustic travel times and low resistivity compared with the normally pressured mudstones. The literature suggests that the overpressure in the Jurassic source rocks is not caused by disequilibrium compaction but by hydrocarbon generation [38]. In summary, three sets of detachment layers, Triassic mudstones, Cretaceous Hutubi Formation mudstones and Paleozoic Anjihaihe Formation mudstones, developed vertically



along the southern Junggar Basin, and the anticline formed in the region is controlled by the three sets of detachment layers.

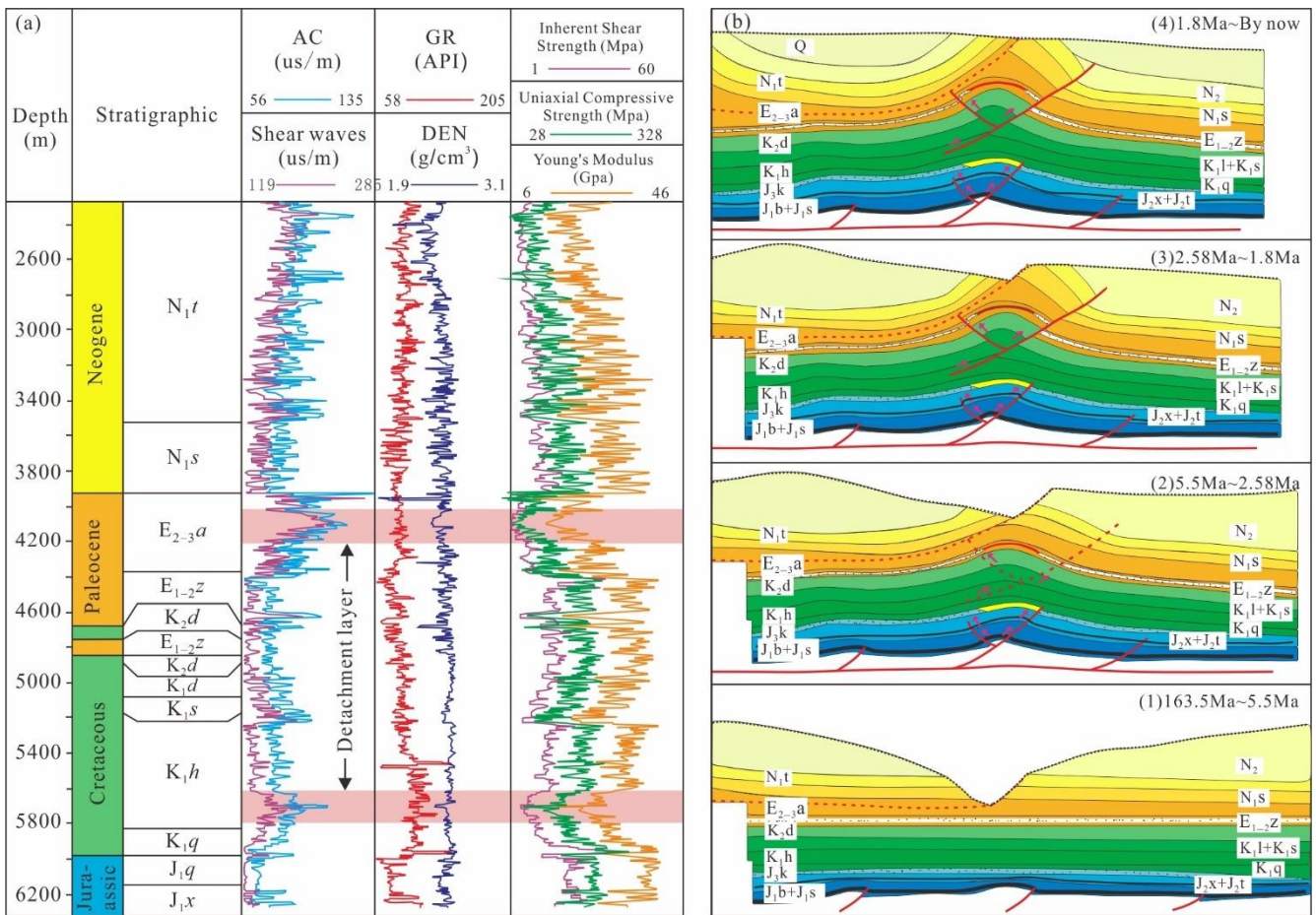


**Figure 3.** Rock mechanics structure columnar section (a) and inversion section of Tulugu anticline model (b) in southern Junggar Basin.

According to the superimposed relationship and stages of tectonics, the anticlines in the southern Junggar Basin can be divided into three types: overthrust anticlines, compound anticlines and multiple superimposed anticlines. In order to improve and ensure the reliability of the tectonic interpretation results, the balanced cross-section recovery technology was used to make the tectonic geological evolution profile to test and correct the tectonic interpretation results in the seismic profile [39]. Using the Tugulu anticline as an example, detachment folds were formed during the Yanshan period. In the Early Himalayan period, the strata formed fault propagation folds along the Cretaceous plastic mudstone and developed thrust faults. In the Middle and Late Himalayan period, the strata formed fault propagation folds along the plastic mudstone of the Anjihaihe Formation and directly broke through the surface, causing the displacement of the middle and shallow anticlines (Figure 3b).

#### 4.2. Characteristics of Typical Tectonic Patterns in Southern Junggar Basin

The characteristics of the three types of anticlines, namely, overthrust anticline, compound anticline and multiple superimposed anticlines, are introduced in turn, mainly including the stratigraphy contained, time of formation, geographical location, and the difficulty of locating.

#### 4.2.1. Overthrust Anticline

An overthrust anticline refers to the development of an anticline in the Middle Petroleum System and Lower Petroleum System, while a syncline develops in the Upper Petroleum System, accompanied by the development of large overthrust faults. The overthrust anticline shows only one anticline stage vertically. The Lower Petroleum System formed low amplitude folds in the Yanshan period, that is, the rudiments of different anticlines in the southern Junggar basin. In the Himalayan period, multi-layer slippage occurred along three sets of thick mudstones of the Upper Triassic, Lower Cretaceous and Anjihaihe Formation. The parts between the anticline belts formed in the Lower Petroleum System are gentle in slope, absorbing the tectonic stress of folding in the Middle and Upper Petroleum System, so no obvious folding can be formed.

Therefore, such anticlines are usually located between different anticline belts in the piedmont. They began to develop in the Yanshan period and finally formed in the Himalayan period. The tectonic highs of this kind of anticline are relatively stable, and it is relatively easy to implement tectonic traps, represented by the Dongwan anticline (Figure 4).

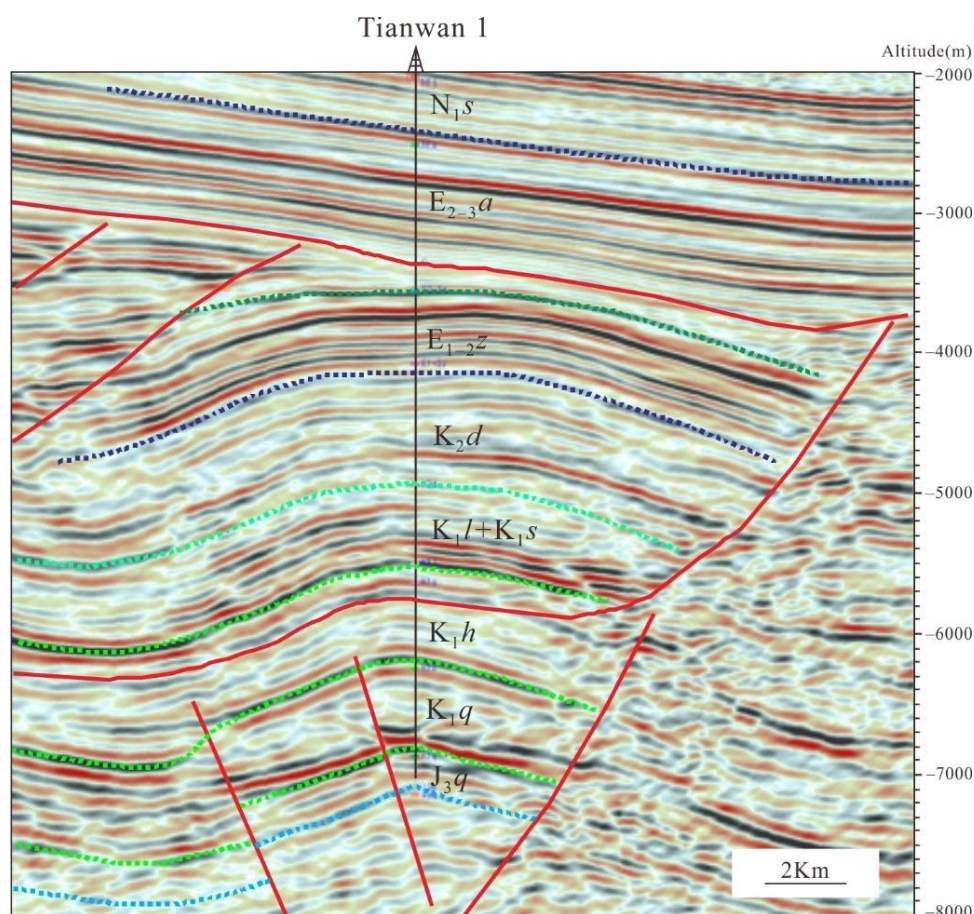


**Figure 4.** Tectonic style section of Dongwan anticline.

Overthrust anticlines are also easily developed in the footwall of the thrust belt near the first row of the anticline belt. Because of the poor quality of seismic data and strong concealment of the tectonic, it is usually called a concealed anticline.

Such anticlines usually occur in groups, and are generally poorly studied. Overthrust anticlines are also developed in the Kuqa area at the southern piedmont of the Tianshan Mountains, which is also of great exploration significance [40].



#### 4.2.2. Compound Anticline

A compound anticline refers to an anticline developed in the Lower Petroleum System, and the anticline also developed in the Middle-Upper Petroleum System, but it shows two stages of anticlines in the vertical direction. This kind of anticline style also began to form in the Yanshan period. The compressive stress in the Himalayan period led to the slippage deformation of the plastic mudstone along the Cretaceous in the middle assemblage. Because the Upper Petroleum System easily absorbs stress and strain and fold, the anticline is developed. This kind of anticline is usually located in the second and third rows of anticline belts, which is far away from the mountain forming belt. At this time, the stress and strain are significantly reduced, and the displacement generated by the anticline is also small, making the deep and shallow tectonic highs consistent. The traps formed by such anticlines have a high degree of implementation. The Hutubi anticline is a compound anticline (Figure 5). Previous studies have shown that from the northern foot of the Tianshan Mountains to the Hutubi anticline, the tectonic displacement decreases from 16.9 km to 0.22 km [3].

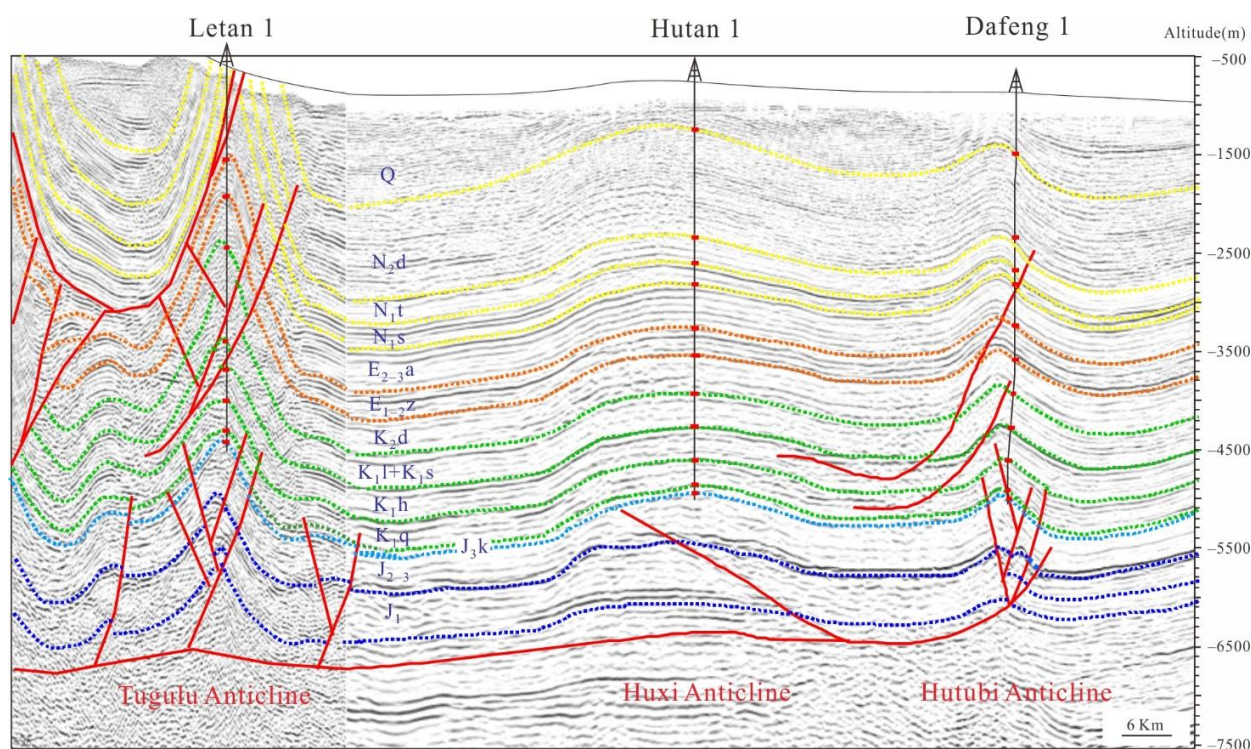


Figure 5. Tectonic style section in southern Junggar Basin.

#### 4.2.3. Multiple Superimposed Anticline

A multiple superimposed anticline means that anticlines were developed in the Lower Petroleum System, and anticlines were also developed in the Middle and Upper Petroleum System and show three stages of anticlines vertically. The anticlines of the three stages overlap each other vertically. This kind of anticline also began to form in the Yanshan period. In the Himalayan period, anticlines were formed in the Middle and Upper Petroleum System due to multi-layer detachment. This kind of anticline is usually located in the first and second rows of anticline belts, which are close to the mountain forming belt. At this time, the stress and strain is large leading to a large displacement of the anticline, making the projection of the tectonic highs on the plane gradually migrate. Generally, the smaller the depth of the anticline, the farther the projection of its tectonic high on the plane from the Tianshan Mountains. As the tectonic highs are gradually migrated, the degree of identification of the traps formed by this kind of anticline is low. This type of anticline includes the Horgos, Manas and Tugulu anticlines (Figure 5). The migration characteristics

of the trap highs in the second row anticline belt in the South Junggar basin have been gradually confirmed by exploration [1,2].

## 5. Discussion

The analysis of the types and characteristics of the tectonic styles in the southern Junggar Basin is intended to explore the characteristics of hydrocarbon accumulation and thus provide guidance for the exploration of hydrocarbons.

### 5.1. Hydrocarbon Accumulation Patterns in Southern Junggar Basin

Based on the understanding of the above tectonic styles, the “multi-stage, vertical stratification” hydrocarbon accumulation model of the multi-slip layer superimposed composite anticline in the southern Junggar basin was constructed (Figure 6). The hydrocarbon of the Lower Petroleum System in the southern Junggar Basin mainly comes from Jurassic and Triassic source rocks [41]. The Triassic Neogene system deposited a very thick sandstone reservoir. The thick mudstone of the Lower Cretaceous is a detachment Layer. At the same time, there is overpressure inside, which provides a good sealing capacity. It is a regional cap rock [42]. Simultaneously, anticline traps of multiple types, multiple stages and large areas are developed, which have the conditions for the formation of large oil and gas fields. However, the tectonic style and its evolution process in the southern Junggar basin is complex. These anticline traps began to develop in the Yanshan period and finally formed after transformation in the Himalayan period, affecting the migration and accumulation of hydrocarbon [43–45]. The time and strata of anticline formation are the main controlling factors for hydrocarbon accumulation [46–50], and the hydrocarbon accumulation conditions for different types of anticlines are different.

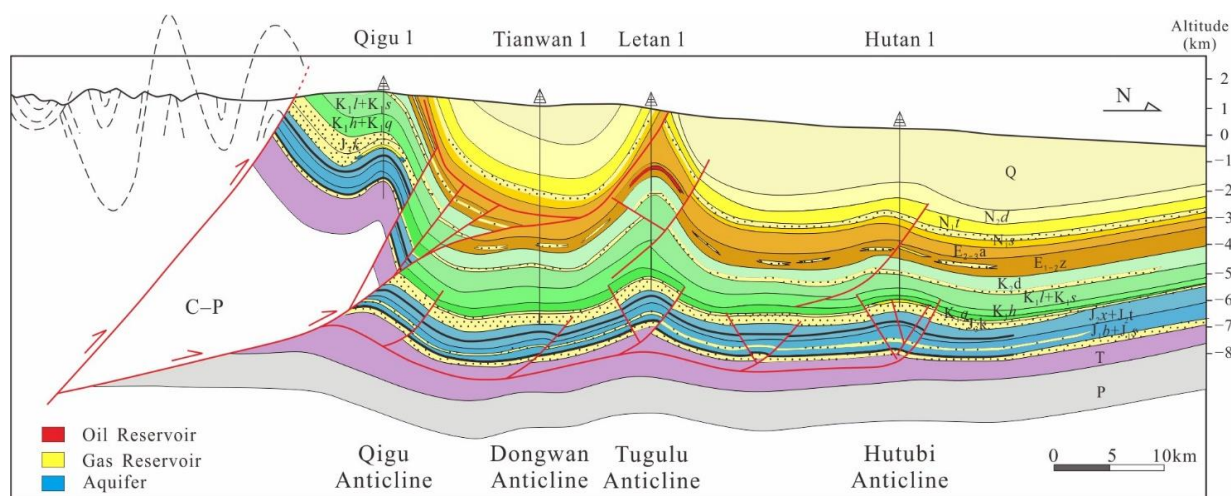


**Figure 6.** Hydrocarbon accumulation model in southern Junggar Basin.

### 5.2. Hydrocarbon Accumulation Characteristics of Different Types of Anticlines

The different formation time and stratigraphy of different types of anticlines imply the variability of hydrocarbon accumulation conditions of different types of anticlines. The comparative analysis of hydrocarbon accumulation characteristics of different types of backslashes is intended to provide guidance for efficient exploration of hydrocarbons in the Lower Petroleum System of southern Junggar Basin.

#### 5.2.1. Reservoir in Overthrust Anticline

Overthrust anticlines are mainly developed in the Lower Petroleum System. The tectonics in the Lower Petroleum System are wider and slower and formed earlier. There are located in the center of highly mature source rock. These are the main areas for hydrocarbon migration and accumulation, mainly gas accumulation (Figure 6). The late



faults are mainly slippage faults, which do not play a role in dredging, so the gas reservoirs formed in the early stage can be well preserved. Hydrocarbon generally comes from deep sources, such as Jurassic and Triassic source rocks. The tectonic highs of overthrust anticlines are relatively stable, but the exploration is difficult due to the deep burial of overthrust anticlines. At present, the Cretaceous Qingshuihe Formation in well Tianwan 1 drilled on the anticline has seen good oil and gas display, and the total hydrocarbon in gas logging has increased from 13,179 ppm to 616,300 ppm. When the gas invaded drilling fluid passed through the liquid–gas separator, the ignition was combustible, and the flame was up to 20 m high and orange, indicating that this kind of anticline has great hydrocarbon potential. The Dongwan Anticline has submitted a probable petroleum initially in place of about  $5.5 \times 10^6$  t.

The concealed overthrust anticlines are usually covered under the middle and shallow thrust faults and are preserved intact. Such anticlines are close to deep hydrocarbon sources and have superior hydrocarbon filling conditions. They often become hydrocarbon-rich tectonics [51]. For example, the Keshen 2 anticline in the Kuqa depression is located in the overthrust anticline at the footwall of the thrust belt, forming the Kelasu gas field [52].

### 5.2.2. Reservoir in Overthrust Anticline

Compound anticlines mainly occur in the second and third rows of the anticline belts in the southern Junggar basin. The compound anticline trap has a relatively high proven degree and favorable reservoir forming conditions. It is the main place for hydrocarbon accumulation and easily forms a multi-layer superimposed “tower type” hydrocarbon reservoir. Both deep and shallow layers can be considered in the development process. The Hutubi anticline began to form in the Yanshan period and experienced three stages of tectonic activity in the Himalayan period. The tectonics change from deep to shallow, and the tectonic stress and deformation degree changes from weak to strong. The large-scale hydrocarbon generation of the main source rocks is within 12 Ma–4 Ma, indicating that the tectonics match the hydrocarbon generation and expulsion time of the source rocks, which is conducive to continuous hydrocarbon filling. Fluid inclusions confirm that the reservoir in Jurassic in well Dafeng 1 experienced early oil and late gas filling and reservoir forming characteristics, and the type of hydrocarbon reservoir is mainly a gas reservoir or condensate gas reservoir (Figure 7). According to the comparative analysis of hydrocarbon sources, the gas in the Hutubi anticline trap comes from the highly mature coal from the Jurassic source rock, and the condensate in the trap comes from the Permian source rock and migrates to the higher part of the anticline through faults to form reservoirs. The Hutubi anticline trap presents a model of “double source hydrocarbon supply, two-stage filling, fault dredging and multi-layer hydrocarbon charging”, which is characterized by rapid hydrocarbon generation and high-efficiency hydrocarbon accumulation.

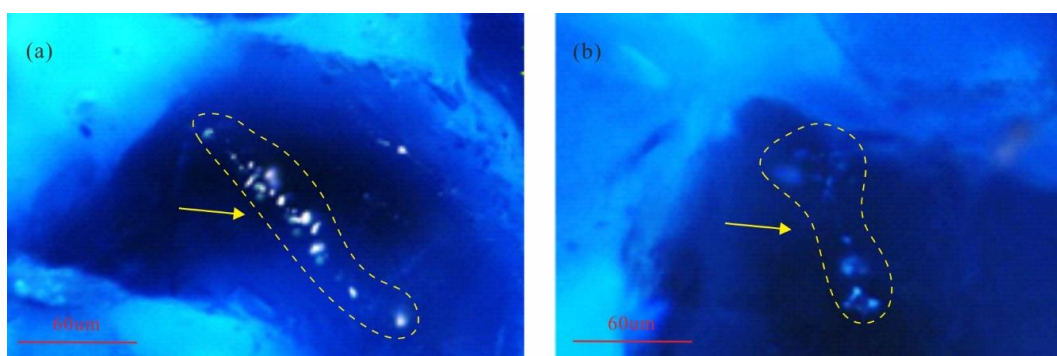


**Figure 7.** Characteristics of fluid inclusions in Hutubi anticline. (a) Fluorescent inclusion, well Dafeng 1, J<sub>3</sub>k, 7114 m, fluorescent thin section. The gas–liquid ratio is about 5%, which is used for early crude oil filling. (b) Fluorescent inclusion, well Dafeng 1, J<sub>3</sub>k, 7116 m, fluorescent thin section. The gas–liquid ratio is about 60–80%, which is the late condensate gas filling.

The exploration history of the Hutubi anticline can be traced back to the 1990s. In 1995, well Hu 2 was drilled, and  $78.3 \times 10^4 \text{ m}^3/\text{d}$  of gas and  $18.82 \text{ m}^3/\text{d}$  of condensate oil were obtained from the Ziniquanzi Formation of the Paleogene, and thus the Hutubi gas field was discovered. In 2012, well Dafeng 1 was deployed for further exploration of the Hutubi anticline and showed abundant oil and gas in the Cretaceous Qingshuihe Formation, which was later abandoned due to engineering reasons. Although no industrial oil and gas breakthrough has been made due to drilling technology and other reasons, drilling has confirmed that thick sandstone layers have been deposited in the Jurassic–Cretaceous system and have formed reservoirs, which has strengthened the confidence for continued exploration of the Jurassic–Cretaceous system.

In 2021, well Hu 6 (Figure 8) was deployed at the east high point of the Hutubi anticline, that is, 2.2 km away from the northwest of the well Dafeng 1. The hydrocarbon display of this well in the Cretaceous and Paleogene was very good, and the thickness of the sandstone forming the gas reservoir is nearly 200 m. When the gas invaded drilling fluid passed through the liquid–gas separator, the ignition was flammable, with orange flame, and the flame height was 7 m, showing great potential for multi-layer hydrocarbon charging in the Hutubi anticline. Later, a probable petroleum initially in place of about  $8 \times 10^6 \text{ t}$  was submitted for the Hutubi anticline.

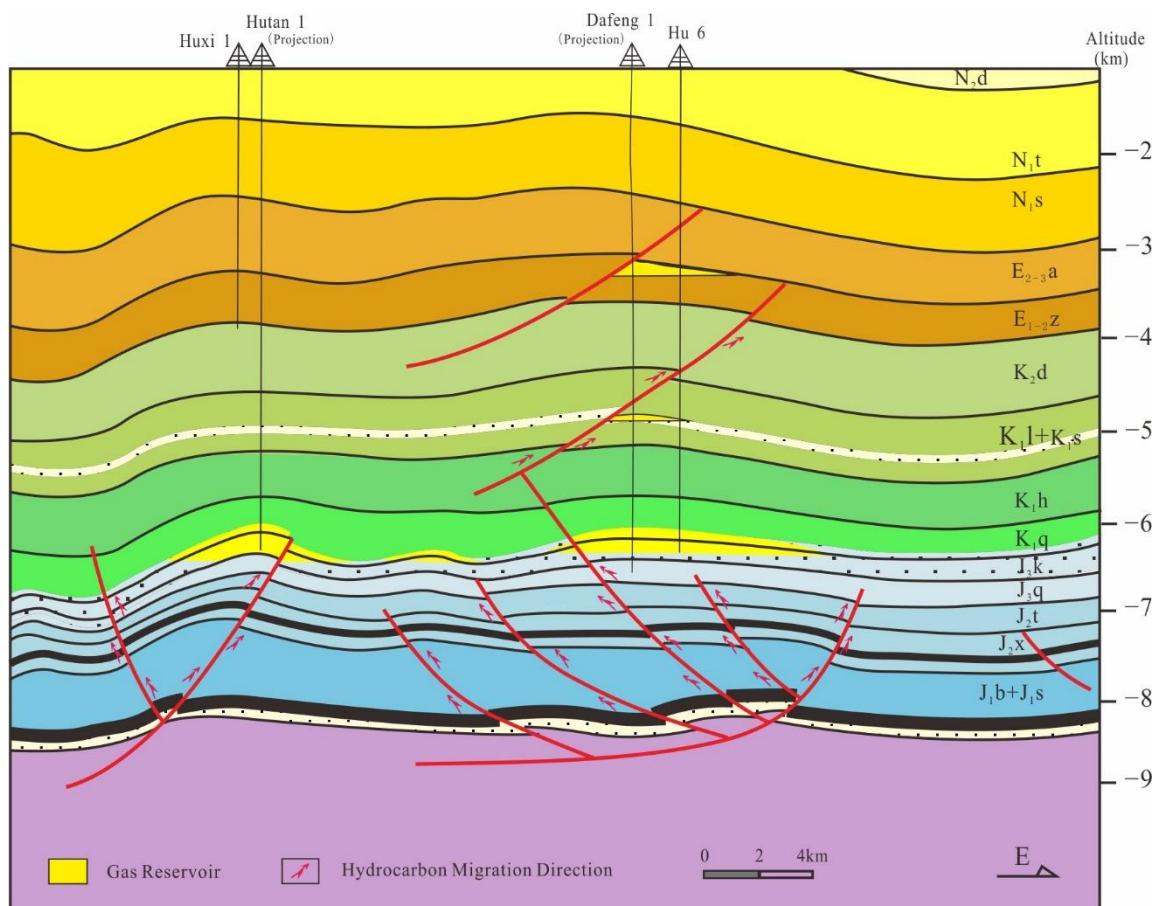


**Figure 8.** Hydrocarbon accumulation model of Hutubi anticline.

### 5.2.3. Reservoir in Multiple Superimposed Anticline

The process of hydrocarbon accumulation in multiple superimposed anticlines is relatively complex. Due to the vertical superimposed development of multiple anticlines, there are multi-layer source rocks and sandstones, matching multi-stage faults, forming a multi-layer reservoir system. Under the sealing action of the decollement layer, the Lower Petroleum System has the best reservoir forming conditions. This kind of anticline style is

a priority exploration object in the early stage. It has a high degree of hydrocarbon filling, and often forms a scene of hydrocarbon enrichment in multiple strata. At the same time, due to the irregular migration of tectonic highs, large dip angles of strata and faults, and complex changes in vertical stress, engineering events should be paid attention to during drilling. Using the Tulugu anticline as an example, three sets of detachment layers are developed in the anticline: Triassic mudstone, Cretaceous Hutubi Formation mudstone and Paleogene Anjihai Formation mudstone. Therefore, it was easy to form deep, middle and shallow thrust faults and folds. The deep strata developed detachment faults along the Triassic mudstone, and the Jurassic and Cretaceous overlying the faults folded, forming the prototype of the Tugulu anticline. The Paleogene Anjihai Formation deposited on the anticline wing is a growth stratum, which indicates that the deep fault activity time is Paleogene. The Tugulu anticline was covered by an unconformity formed in the Neogene, indicating that deep faults ceased to be active during the Neogene. In the Miocene, the Huomatu fault developed along the mudstone of the Anjihai Formation of the Paleogene. The fault thrust northward, cut through the top of the deep anticline, and was exposed to the surface. The shallow Tugulu anticline developed in the hanging wall of the fault and was superimposed on the deep anticline, presenting a “three-layer tower” tectonic style as a whole. The Tugulu oil reservoir was discovered in the Middle Petroleum System of the anticline in 2003. In 2019, well Letan 1 was drilled for the Lower Petroleum System. The well shows rich hydrocarbon, and low hydrocarbon production was obtained during oil test. The oil test results confirmed that hydrocarbons have accumulated in the Lower Petroleum System formed reservoirs. Later, a probable petroleum initially in place of about  $2.5 \times 10^6$  t was submitted for the Tugulu anticline. Affected by the seismic data, the traps developed in the lower assemblage of the Tugulu anticline are relatively poorly implemented, resulting in the drilling of well Letan 1 to the wings of the anticline (Figure 6).

## 6. Conclusions

There are many anticlines in the southern margin of the Junggar Basin, which can be divided into overthrust anticlines, compound anticlines and multiple superimposed anticlines according to the superposition relationship and the formation stages of the tectonics. Overthrust anticlines are developed in the Lower Petroleum System between anticline belts, compound anticlines are developed in the second row and third row of the anticline belts, and multiple superimposed anticlines are developed in the first and second rows of anticline belts.

The hydrocarbon accumulation conditions of compound anticlines are the best, especially the Hutubi anticline. A probable petroleum initially in place of about  $8 \times 10^6$  t was submitted for the Hutubi anticline. The anticline formed a detachment fold in the Yanshan period, and the deformation was further strengthened along the Cretaceous plastic mudstone in the Himalayan period, so that the plane projection of the deep and shallow tectonic highs basically coincided. This kind of anticline has the characteristics of “double source hydrocarbon supply, two-stage filling, fault dredging and multi-layer hydrocarbon charging”. It has great hydrocarbon potential and can be exploited simultaneously in multiple layers during the development process.

**Author Contributions:** Conceptualization, D.J., Y.X. and K.Z.; methodology, D.J. and Y.X.; software, Z.P., B.Y. and K.Z.; validation, D.J. and Y.X.; formal analysis, D.J.; investigation, D.J. and Y.X.; resources, D.J.; data curation, Z.P. and B.Y.; writing—original draft preparation, D.J.; writing—review and editing, D.J. and K.Z.; visualization, D.J. and K.Z.; supervision, B.Y. All authors have read and agreed to the published version of the manuscript.

**Funding:** This research was funded by Major Science and Technology Project, PetroChina, grant number 2021DJ2101.

**Data Availability Statement:** Not applicable.



**Acknowledgments:** We are grateful to the Research Institute of Petroleum Exploration and Development, PetroChina Xinjiang Oilfield, for permission to access their in-house database, providing geologic data and permission to publish the results.

**Conflicts of Interest:** The authors declare no conflict of interest.

## References

1. Shao, Y. Hydrocarbon Accumulation of the Jurassic Deeply-buried Lower Assemblage in the Southern Junggar Basin. *Geol. J. China Univ.* **2013**, *19*, 86–94.
2. Ma, D.L.; He, D.F.; Wei, D.T.; Wang, Y.J.; Wei, C.R. Multiple Phase Deformation of Gumudi Anticline at South Margin of Junggar Basin. *J. Jilin Univ. (Earth Sci. Ed.)* **2017**, *47*, 1695–1704.
3. Guan, S.W.; Li, B.L.; He, D.F.; Wang, X.; John, S. Geometrical Methods of Complicated Tectonic Analysis and their Application. *Chin. J. Geol.* **2007**, *42*, 722–739.
4. Guan, S.W.; Li, B.L.; He, D.F.; Shaw, J.H.; Chen, Z.X. Recognition and Exploration of Tectonic Wedges—A Case Study of the Southern margin of Junggar Basin. *Earth Sci. Front.* **2009**, *16*, 129–137. [[CrossRef](#)]
5. Guan, S.W.; Plesch, A.; Li, B.L.; Chen, Z.X.; He, D.F. Volumetric tectonic restorations based on mechanical constraints and its geological Significance. *Earth Sci. Front.* **2010**, *17*, 140–150.
6. Guan, S.W.; Chen, Z.X.; Fang, S.H. Three potential exploration areas of Southern Junggar Basin: Arguments from tectonic modeling. *Pet. Explor. Dev.* **2012**, *39*, 37–44. [[CrossRef](#)]
7. Kuang, L.C.; Wang, X.L.; Zhang, J.; Xia, H.P. Tectonic modeling of the Huoerguoshi-Manashi-Tugulu thrust belt at the southern margin of the Junggar Basin and the discovery of the Mahe Gas Field. *Nat. Gas Ind.* **2012**, *32*, 11–15.
8. Lei, D.W.; Zhang, J.; Chen, N.G.; Xiang, B.L. Conditions for gas pooling in the lower assemblage in the southern margin of the Junggar Basin and the exploration prospect of large hydrocarbon fields. *Nat. Gas Ind.* **2012**, *32*, 16–22.
9. Li, B.L.; Guan, S.W.; Chen, Z.X.; Shaw, J.H.; Lei, Y.L.; Wang, L.N.; Zhao, X. The Effect of Wedge Structure on Displacement Subduction of Piedmont Thrust Structure: A Case Study of the Southern Margin of Junggar Basin. *Acta Geol. Sin.* **2012**, *86*, 890–897.
10. Peng, T.L.; Yan, G.H.; Chen, W.; Xiao, L.X. Characteristics of Huoerguosi-Manasi-Tugulu Tectonic Belt in Junggar Basin. *Xinjiang Pet. Geol.* **2008**, *29*, 191–194.
11. Chen, W.; Hao, J.J.; Zhang, J.; Xiao, L.X.; Xian, D.; Li, Z.G.; Chen, L.H.; Li, G.Z. Geometrical kinematics of the Tuositai Anticline in the southern margin of the Junggar Basin. *Acta Pet. Sin.* **2011**, *32*, 90–94.
12. Xiao, L.X.; Lei, D.W.; Wei, L.Y.; Zheng, X.M.; Yan, G.H. Tectonic types and features in the west of south margin in the Junggar Basin. *Nat. Gas Ind.* **2012**, *32*, 36–39.
13. Wang, Y.J.; Wei, D.T.; Pan, J.G.; Liu, Z.H.; Zhang, J.; Li, L.X. The Determination of Geometric and Kinematic Parameters for the Dushanzi Anticline in Southern Margin of Junggar Basin and Its Significance. *Geol. J. China Univ.* **2012**, *18*, 711–718.
14. Wang, X.X.; Liu, Y.M.; Hou, J.G.; Li, S.H.; Kang, Q.Q.; Sun, S.; Ji, L.; Sun, J.; Ma, R. The relationship between syndepositional fault activity and reservoir quality—A case study of the Ek1 formation in the Wang Guantun area, China. *Interpretation* **2020**, *8*, 15–24. [[CrossRef](#)]
15. Wang, X.X.; Zhou, X.R.; Li, S.H.; Zhang, N.D.; Ji, L.; Lu, H. Mechanism Study of Hydrocarbon Differential Distribution Controlled by the Activity of Growing Faults in Faulted Basins: Case Study of Paleogene in the Wang Guantun Area, Bohai Bay Basin, China. *Lithosphere* **2022**, 7115985. [[CrossRef](#)]
16. Wang, X.X.; Zhang, F.; Li, S.H.; Dou, L.X.; Liu, Y.M.; Ren, X.X.; Chen, D.P.; Zhao, W. The Architectural Surfaces Characteristics of Sandy Braided River Reservoirs, Case Study in Gudong Oil Field, China. *Geofluids* **2021**, *2021*, 8821711. [[CrossRef](#)]
17. Wang, Y.J.; Jia, D.; Pam, J.G.; Wei, D.T.; Tang, Y.; Wang, G.D.; Wei, C.R.; Ma, D.L. Multiple-phase tectonic superposition and reworking in the Junggar Basin of northwestern China—Implications for deep-seated petroleum exploration. *AAPG Bull.* **2018**, *102*, 1489–1521. [[CrossRef](#)]
18. Guan, S.W.; Stockmeyer, J.M.; Shaw, J.H.; Plesch, A.; Zhang, J. Structural inversion, imbricate wedging, and out-of-sequence thrusting in the southern Junggar fold-and-thrust belt, northern Tian Shan, China. *AAPG Bull.* **2016**, *100*, 1443–1468. [[CrossRef](#)]
19. He, H.Q.; Zhi, D.M.; Yang, D.S.; Xiao, L.X.; Yuan, B.; Qi, X.F.; Zhao, J.Y. Strategic breakthrough in Gaoquan Anticline and Exploration assessment on lower assemblage in the southern margin of Junggar Basin. *China Pet. Explor.* **2019**, *24*, 137–146.
20. Li, X.Y.; Shao, Y.; Li, T.M. Three oil-reservoir combinations in south marginal of Junggar Basin, Northwest China. *Pet. Explor. Dev.* **2003**, *30*, 32–34.
21. Li, Y.H. Natural gas pool formation models and exploration direction in South Junggar Basin. *Nat. Gas Ind.* **2001**, *21*, 27–31.
22. Li, T.J.; Wang, T.D.; Zhang, Y.Y.; Chen, S.J.; Wang, X.L. Natural Gas Genesis and Formation of Gas Pools in the South Margin of Junggar Basin. *Acta Sedimentol. Sin.* **2004**, *22*, 529–534.
23. Wu, X.Q.; Huang, S.P.; Liao, F.R.; Li, Z.S. Geochemical Characteristics and Sources of Natural Gas from the South Margin of Junggar Basin. *Nat. Gas Geosci.* **2011**, *22*, 224–232.
24. Guo, J.G.; Wang, X.L.; Pang, X.Q.; Lei, D.W.; Xiang, C.F.; Long, H.S.; Gao, S. Evaluation and hydrocarbon expulsion characteristics of the Middle-Lower Jurassic source rock in the southern margin of Junggar Basin. *J. China Univ. Min. Technol.* **2013**, *42*, 595–605.

25. Chen, J.P.; Wang, X.L.; Deng, C.P.; Zhao, Z.; Ni, Y.Y.; Sun, Y.G.; Yang, H.B.; Wang, H.T.; Liang, D.G.; Zhu, R.K.; et al. Geochemical features of source rocks in the southern margin, Junggar Basin, Northwestern China. *Acta Pet. Sin.* **2015**, *36*, 767–780.
26. Chen, J.P.; Wang, X.L.; Deng, C.P.; Zhao, Z.; Ni, Y.Y.; Sun, Y.G.; Yang, H.B.; Wang, H.T.; Liang, D.G. Oil-source correlation of typical crude oils in the southern margin, Junggar Basin, Northwestern China. *Acta Pet. Sin.* **2016**, *37*, 160–171.
27. Chen, J.P.; Deng, C.P.; Wang, X.L.; Ni, Y.Y.; Sun, Y.G.; Zhao, Z.; Liao, J.D.; Wang, P.R.; Zhang, D.J.; Liang, D.G. Formation mechanism of condensate, waxy oil and heavy oil at the southern edge of Junggar Basin. *Sci. Sin. (Terrae)* **2017**, *47*, 567–585.
28. Chen, J.P.; Wang, X.L.; Ni, Y.Y.; Xiang, B.L.; Liao, F.R.; Liao, J.D.; Zhao, C.Y. Genetic type and source of natural gas in the southern margin of Junggar Basin, NW China. *Pet. Explor. Dev.* **2019**, *46*, 461–473. [[CrossRef](#)]
29. Chen, J.P.; Wang, X.L.; Ni, Y.Y.; Xiang, B.L.; Liao, F.R.; Liao, J.D. The accumulation of natural gas and potential exploration regions in the southern margin of the Junggar basin. *Acta Geol. Sin.* **2019**, *93*, 1002–1019.
30. Du, J.H.; Zhi, D.M.; Li, J.Z.; Yang, D.S.; Tang, Y.; Qi, X.F.; Xiao, L.X.; Wei, L.Y. Major breakthrough of Well Gaotan 1 and exploration prospects of lower assemblage in southern margin of Junggar Basin, NW China. *Pet. Explor. Dev.* **2019**, *46*, 205–215. [[CrossRef](#)]
31. Xiao, Q.L.; He, S.; Yang, Z.; He, Z.L.; Furong, W.; Li, S.F.; Tang, D.Q. Petroleum secondary migration and accumulation in the central Junggar Basin, northwest China: Insights from basin modeling. *AAPG Bull.* **2010**, *94*, 937–955. [[CrossRef](#)]
32. Gui, R.; Wan, Y.P. Rock mechanics parameter calculation based on conventional logging data: A case study of Upper Paleozoic in Ordos Basin. *J. Geomech.* **2012**, *18*, 418–424.
33. Zhang, G.J.; Wu, K.Y.; Fan, C.L.; Liu, J.S.; Deng, G.J.; Liu, Y.J. Calculation and Significance of Rock Mechanical Parameters of Deeply-buried Miocene Reservoir Rocks in the Key Offshore Exploration Blocks of the Yingqiong Basin. *China Geol. J. China Univ.* **2021**, *27*, 616–624.
34. Epard, J.L.; Groshong, R.H. Excess area and depth to detachment. *AAPG Bull.* **1993**, *77*, 1291–1302.
35. Groshong, R.H. Area balance, depth to detachment, and strain in extension. *Tectonics* **1994**, *13*, 1488–1497. [[CrossRef](#)]
36. Qi, J.F.; Groshong, R.H.; Yang, Q. Analysis method for predicting strain of interior beds and sub-resolution faults from Area-Balance Theory in Extensional Basin. *Earth Sci.* **2002**, *6*, 696–702.
37. Zhang, Y.P.; Zhang, J.; Yin, H.W.; Xu, S.J. The regional detachment of Dachigan thrust belt, Eastern Sichuan: Results from geological section restoration based on Area-Depth Technique. *Geotecton. Et Metallog.* **2008**, *4*, 410–417.
38. Guo, X.W.; He, S.; Liu, K.Y.; Yang, Z.; Yuan, S.Q.; Liu, M.L. Generation and evolution of overpressure caused by hydrocarbon generation in the Jurassic source rocks of the central Junggar Basin, northwestern China. *AAPG Bull.* **2019**, *103*, 1553–1574. [[CrossRef](#)]
39. He, D.F.; John, S.; Jia, C.Z. New advances in theory and application of fault-related folding. *Earth Sci. Front.* **2005**, *12*, 353–364.
40. Lu, X.S.; Liu, K.Y.; Zhuo, Q.G.; Zhao, M.J.; Liu, S.B.; Fang, S.H. Palaeo-fluid evidence for the multi-stage hydrocarbon charges in Kela-2 gas field, Kuqa foreland basin, Tarim Basin. *Pet. Explor. Dev.* **2012**, *39*, 537–544. [[CrossRef](#)]
41. Ren, J.L.; Wang, F.Y.; Zhao, Z.Y.; Zhang, Y.P.; Mi, J.L.; Liu, C.M. Genesis of Oil and Gas in Sikeshu Sag in the Southern Margin of Junggar Basin. *Xinjiang Pet. Geol.* **2020**, *41*, 25–30.
42. Zhang, W.L.; Zhang, X.N.; Chen, Y.C.; Wang, S.Q. Analysis of formation overpressures in the west part of Zhunnan region. *Nat. Gas Ind.* **2004**, *24*, 26–28.
43. Kang, Y.S.; Zhang, Y.W. *Hydrodynamics of Hydrocarbon Accumulation*; Geology Press: Beijing, China, 1999; pp. 154–158.
44. Li, X.Y.; Wang, B.; Chen, Y. Fracture mode and oil control of the mountain front fold belt in the southern margin of the Junggar Basin. *Xinjiang Pet. Geol.* **2006**, *27*, 285–287.
45. Chen, T.; Wei, D.T.; Yang, H.B.; Wu, L.Y. The tectonic characteristics of the Foreland Thrust Belt and its influence on reservoiring of oil and natural gas Southern Junggar Basin. *Nat. Gas Geosci.* **2006**, *17*, 711–718.
46. Luo, X.R.; Xiao, L.X.; Li, X.Y.; Zhang, L.Q.; Zeng, Z.P. Overpressure distribution and affecting factors in southern margin of Junggar Basin. *Earth Sci.* **2004**, *29*, 404–412.
47. Chen, Y.; Wang, X.T.; Fang, S.H.; Zhang, J.; Zhao, M.J.; Liu, S.B.; Bai, Z.H. Hydrodynamic characteristics of hydrocarbon accumulation in E1-2z of Huo-Ma-Tu tectonic belt, southern Junggar Basin, NW China. *J. China Univ. Pet. (Ed. Nat. Sci.)* **2013**, *37*, 30–36.
48. Bai, Z.H.; Jiang, Z.X.; Song, Y.; Zhao, M.J.; Fang, S.H.; Zhang, J. The Reservoir Characteristics and Its Main Controlling Factor Discussion in Ziniquanzi Formation of Huomatu Tectonic Zone, Southern Junggar Fold-thrust Belt. *Nat. Gas Geosci.* **2013**, *24*, 273–281.
49. Bai, Z.H.; Jiang, Z.X.; Song, Y.; Fang, S.H.; Zhao, M.J. The main controlling factor of oil-gas-water distribution and its implications in Huomatu tectonic zone of southern Junggar thrust Belt. *J. Oil Gas Technol.* **2013**, *35*, 40–44.
50. Hu, H.W.; Zhang, Y.Y.; Zhuo, Q.G.; Jia, C.Z.; Guo, Z.J. Hydrocarbon charging history of the lower petroleum system in the southern Junggar Basin: Case study of the Qigu Oil Field. *Nat. Gas Geosci.* **2019**, *30*, 456–467.
51. Guan, S.W.; Li, B.L.; Hou, L.H.; He, D.F.; Shi, X.; Zhang, Y.Q. New hydrocarbon exploration areas in footwall covered structures in northwestern margin of Junggar Basin. *Pet. Explor. Dev.* **2008**, *1*, 17–22. [[CrossRef](#)]
52. Du, J.H.; Wang, Z.M.; Hu, S.Y.; Wang, Q.H.; Xie, H.W. Formation and geological characteristics of deep giant gas provinces in the Kuqa foreland thrust belt, Tarim Basin, NW China. *Pet. Explor. Dev.* **2012**, *39*, 385–393. [[CrossRef](#)]